PNAS
www.pnas.org

Supplementary Information for

A cancer-associated polymorphism in ESCRT-III disrupts the abscission checkpoint and promotes genome instability

Jessica B.A. Sadler[1†], Dawn M. Wenzel[2†], Lauren K. Strohacker[2,7], Marta Guindo-Martínez[3], Steven L. Alam[2], Josep M. Mercader[3,4,5], David Torrents[3,6], Katharine S. Ullman[7], Wesley I. Sundquist[2]* and Juan Martin-Serrano[1]*.

Wesley I. Sundquist and Juan Martin-Serrano
Email: wes@biochem.utah.edu, juan.martin_serrano@kcl.ac.uk.

This PDF file includes:

Supplementary text
Figs. S1 to S10
Tables S1 to S2
Captions for Movies S1 to S23
References for SI reference citations

Other supplementary materials for this manuscript include the following:

Movies S1 to S23

www.pnas.org/cgi/doi/10.1073/pnas.1805504115

Supplementary Information Text

Methods:

Protein expression and purification:

The human ALIX Bro1 domain (residues 1-359, Fig. 1*C*, *D*, Fig. S1) and ALIX Bro1-V domains (residues 1-698, Fig. 1*B*) were expressed and purified as previously described with minor modifications(1, 2). Briefly, ALIX Bro1 and ALIX Bro1-V were expressed as His-tagged proteins in BL21- CodonPlus (DE3)-RIPL E. Coli (Agilent, Santa Clara, CA) using ZYP-5052 auto-induction media (3). All subsequent steps were performed at 4°C. Cells were pelleted and lysed by sonication in 50 mM Tris, pH 8.0, 500 mM NaCl, 1 mM DTT, 0.5 mM EDTA in the presence of 0.125% sodium deoxycholate, protease inhibitors (Leupeptin, Pepstatin, PMSF and Aprotinin), DNAse I (Roche) and Lysozyme (Sigma). Lysates were clarified by centrifugation (29,000 x g for 45 minutes), filtered using a 0.45 μM filter, and incubated with cOmplete His-tag purification resin (Roche) for 20 minutes. Resin was washed with 20 column volumes of lysis buffer and bound proteins were eluted with 5 column volumes of lysis buffer containing 250 mM imidazole. The eluate was dialyzed twice against 4 L of 25 mM Tris, pH 8.0, 50 mM NaCl, 1 mM DTT, 0.5 mM EDTA at 4°C. For ALIX Bro1-V, dialysis was performed in the presence of ~1 mg TEV protease, to remove the His tag. The His tag on ALIX Bro1 was not removed, as it improves crystallization when present. Cleaved ALIX Bro1-V was re-incubated with cOmplete His-tag purification resin to remove the His tag and residual un-cleaved protein.

All proteins were further purified by anion exchange chromatography on a Q-sepharose column (GE Healthcare Life Sciences) in 25 mM Tris, pH 8.0 eluting over a gradient from 0.05-1 M NaCl over 7 column volumes. Under these buffer conditions, ALIX Bro1 does not bind to the Q sepharose column, whereas ALIX Bro1-V binds and is eluted during the NaCl gradient. ALIX protein-containing fractions were pooled, concentrated and further purified by size exclusion chromatography using a Superdex 75 column (GE) ALIX Bro1: 10 mM Tris, pH 8.0, 100 mM NaCl, 1 mM DTT) or a Superdex 200 column (GE) (ALIX Bro1-V: 20 mM sodium phosphate, pH 7.2, 150 mM NaCl, 5 mM BME). Pure ALIX protein-containing fractions were pooled, concentrated and used for binding or crystallographic studies. Typical yields were 8-10 mg/L culture (ALIX Bro1-V), and 15-20 mg/L culture (ALIX Bro1).

GST pull-down assay:
GST-fused CHMP4C peptides spanning the ALIX binding helix (residues 216-233) from $CHMP4C^{A232}$ or the $CHMP4C^{L228A,W231A}$ or $CHMP4C^{T232}$ mutants were expressed in BL21 *E. coli* by IPTG induction (0.5 mM) for 4 hours at 37°C. Cells were harvested, resuspended in bacterial lysis buffer (50 mM Tris, pH 7.4, 100 mM NaCl, 1 mM EDTA), Protease Inhibitor Cocktail (Roche), and Lysozyme (1 mg/mL) and sonicated. Lysates were clarified by centrifugation at 28,000 x g for 30 minutes, proteins were immobilized on glutathione-Sepharose 4ß resin, and unbound protein was removed by repeated washes in 50 mM Tris, pH 7.4, 100 mM NaCl, 1 mM EDTA. Bound protein quantities were determined by SDS-PAGE and Coomassie staining. Equal protein quantities of GST or GST-CHMP4C fusions bound to glutathione-Sepharose were incubated with 1 ml of 1 mg/ml clarified HeLa cell lysate for 3 hours with rotation at 4°C in binding buffer: 50 mM Tris-HCl, pH 7.4, 150 mM NaCl, 5 mM EDTA, 5% glycerol, 1% Triton X-100. HeLa cells were grown as described, lysed in binding buffer by sonication, clarified by centrifugation and protein content was determined using microBCA kit (Thermo Scientific). Following incubation with GST-CHMP4C fusion proteins, unbound proteins were removed by four washes with 50 mM Tris-HCl, pH 7.4, 150 mM NaCl, 5 mM EDTA, 5% glycerol, 0.1% Triton X-100. Bound proteins were eluted with Laemelli sample buffer and analyzed by SDS-PAGE followed by immunoblotting or Coomassie staining.

Yeast two-hybrid assay:
Yeast two-hybrid assays were carried out as described previously (4). Briefly, full-length CHMP4C proteins were fused to the VP16 activation domain (pHB18) and full-length binding partners (ALIX or CHMP4C) were fused to Gal4 DNA binding domain (pGBKT7). Yeast Y190 cells were co-transformed with plasmids and grown under selection with SD-Leu-Trp for 3 days at 30°C. Cells were harvested and LacZ activity was measured with a liquid β -galactosidase assay using chlorophenol-red-β-D-galactopyranoside (Roche) as a substrate.

CRISPR deletion of the CHMP4C locus:
CRISPR guides targeting the CHMP4C gene immediately prior to the start and following the stop codon were designed using **http://crispr.mit.edu/** (5). Guide RNA sequences were TCGGAGGGCCAGCGATCCCG and TGCATACATAGAATCAGTGA. These were cloned into a Cas9 containing GFP lentiviral packaging vector (pLG2C). Target HCT116 cell lines were co-transfected with both guides for 48 hours. Single cells expressing vectors were isolated by fluorescence-activated cell sorting based on GFP fluorescence and cultured until ready for screening. The CHMP4C status of CRISPR-treated clones was determined at the mRNA level using Qiagen RNeasy kit followed by cDNA synthesis (Applied Biosystems), and PCR. The CHMP4C status of clones was also determined at the genomic level using DNeasy Blood and Tissue kit (Qiagen) followed by PCR. Primers used in this study are available in Table S2. Protein expression was determined by immunoblotting (Fig. S3).

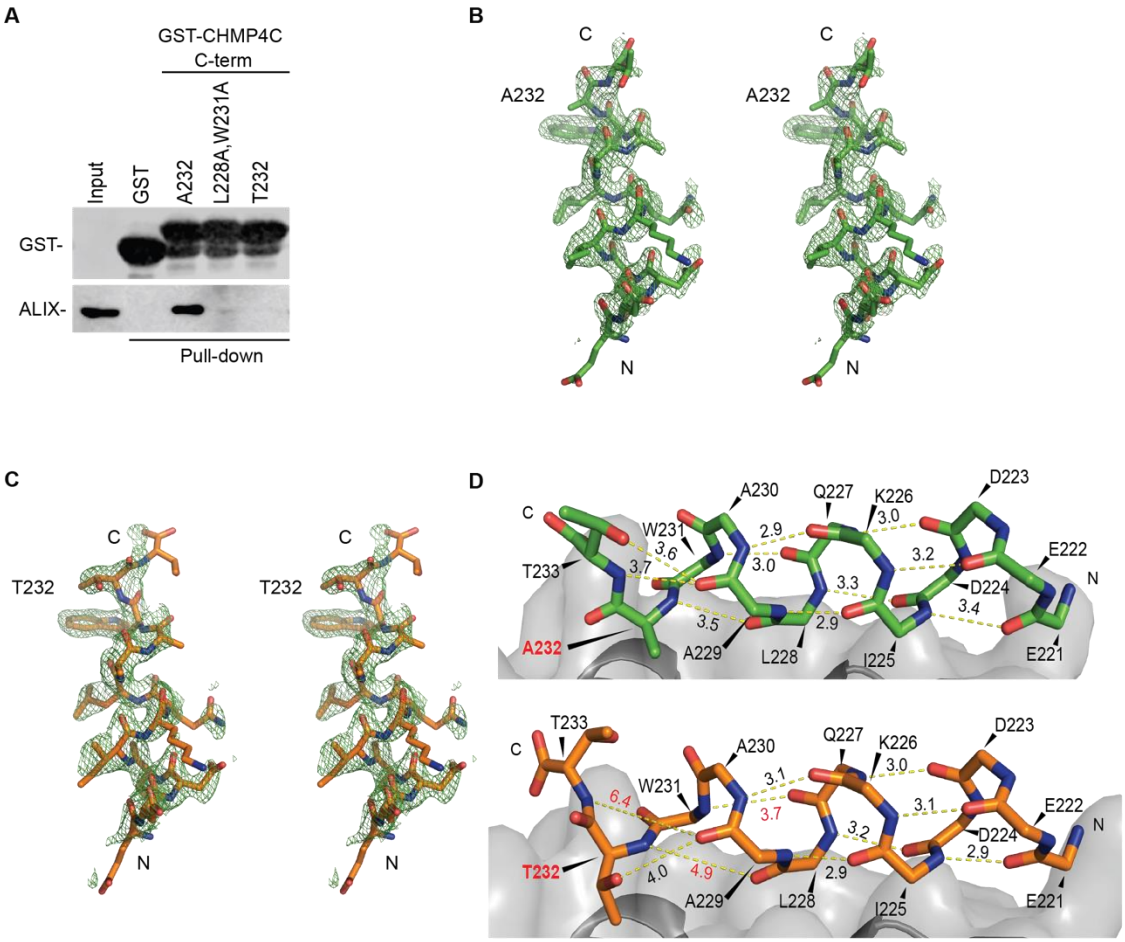

Fig. S1. The CHMP4C A232T substitution reduces binding to the ALIX adapter protein. (**A**) Endogenous ALIX protein precipitated from HeLa cell lysates with the indicated C-terminal CHMP4C peptides (residues 216-233) fused to GST, or with GST alone. (**B**, **C**) Stereoviews showing unbiased CHMP4C peptide density in Fo-Fc omit maps (green mesh, contoured at 2.0 σ) superimposed on the final structural models for the ALIX/CHMP4C^{A232} (**B**) and ALIX/CHMP4C^{T232} (**C**) complexes. (**D**) Comparison of the i+4 helical hydrogen bonding patterns for ALIX-bound CHMP4C^{A232} (top, green) and CHMP4C^{T232} (bottom, orange) peptides. For clarity, all side chains except for T232/A232 and T233 have been removed. Note that the T232 polymorphism breaks: 1) the final two backbone helical hydrogen bonds (Q227(CO)---W231(N) is 3.0 Å in CHMP4C^{A232} vs. 3.7 Å in CHMP4C^{T232} and L228(CO)---A/T232(N) is 3.5 Å in CHMP4C^{A232} vs. 4.9 Å in CHMP4C^{T232}), and 2) The C-terminal helix capping interaction (T233(Oγ)--- A229(CO) is 3.6 Å in CHMP4C^{A232} vs. 6.4 Å in CHMP4C^{T232}). Broken hydrogen bond distances are shown in red font in the bottom panel**.**

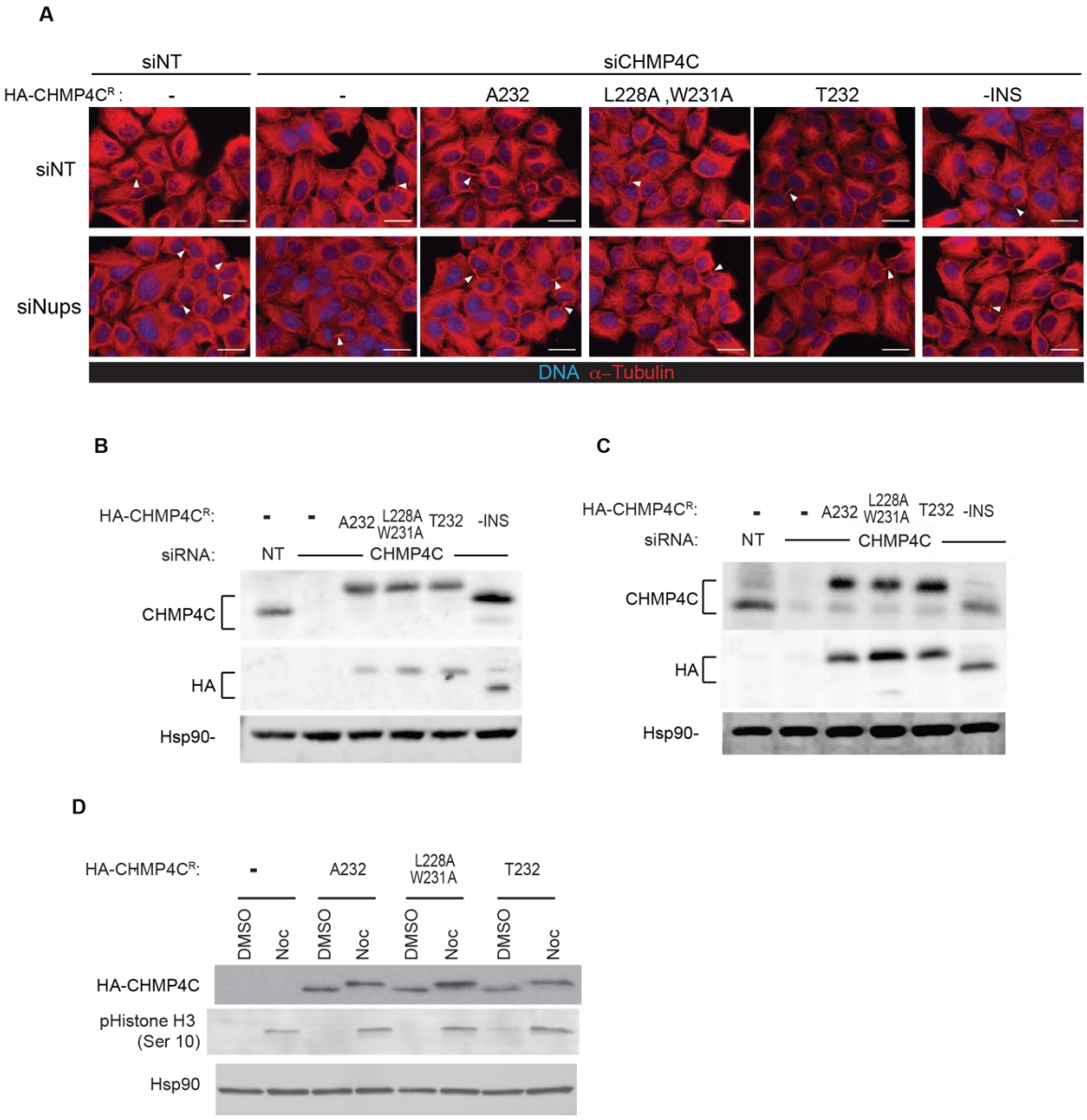

Fig. S2. CHMP4C T232 does not support the abscission checkpoint.
(**A**) Cells stably expressing the indicated HA-CHMP4C constructs and treated with the indicated siRNA stained for α-tubulin (red) and DNA (blue). Cells connected with midbodies are marked with arrow heads. Scale bars are 20 μm. (**B, C**) Representative immunoblots of cell lines used in Fig. 2*B* (**B**) and Fig. 2*C* (**C**). (**D**) Immunoblots showing comparable mitotic phosphorylation of the indicated HA-CHMP4C constructs following mitotic arrest using a double thymidine-nocodazole block.

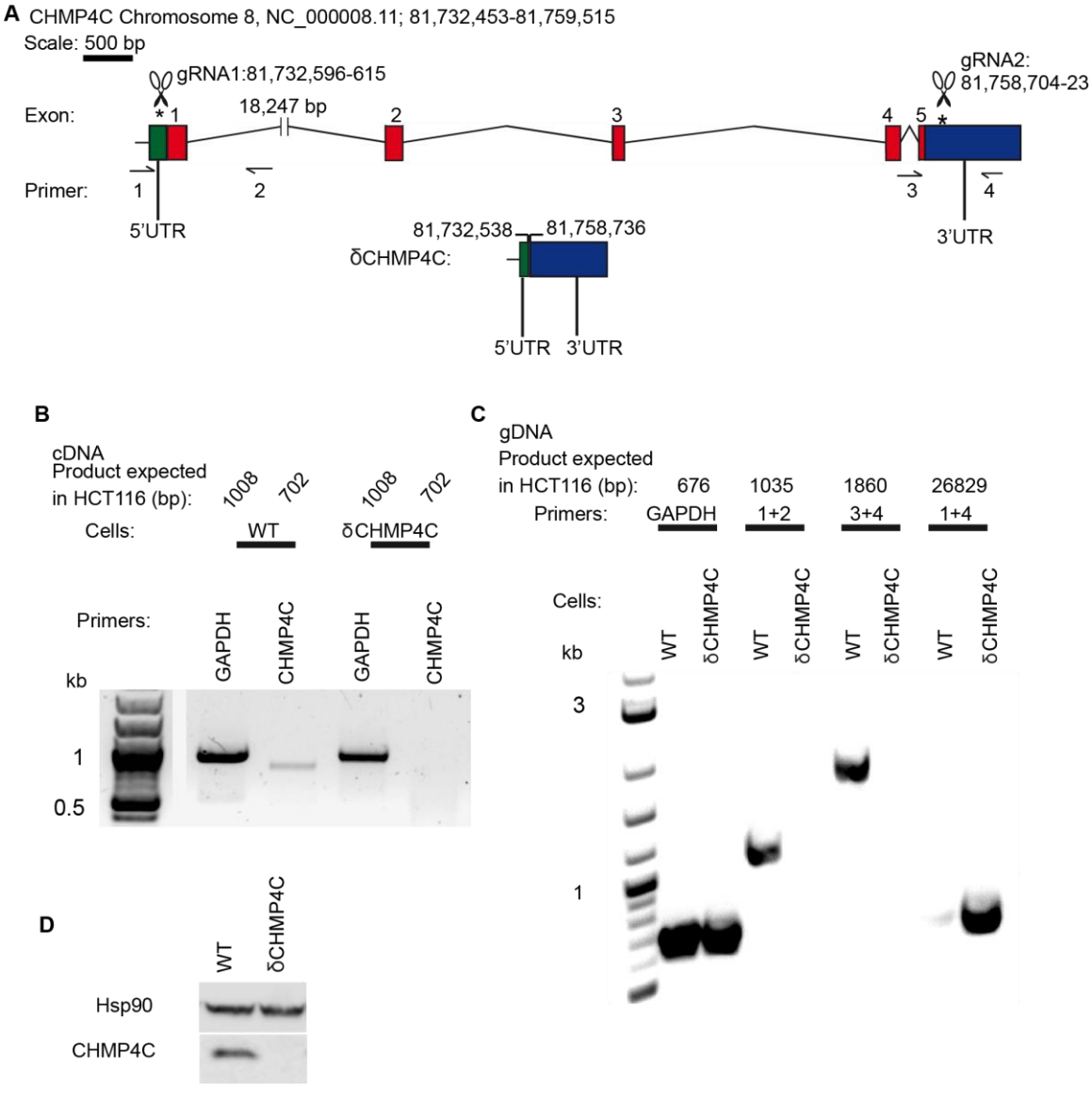

Fig S3. Generation of δCHMP4C cell lines.

(**A**) Schematic of the CHMP4C gene showing guide RNA and primer locations. Analysis of CHMP4C deletion was carried out at the cDNA (**B**), genomic (**C**) and protein (**D**) levels. (**E**) The residual CHMP4C locus in the HCT116$^{\delta CHMP4C}$ cell line was amplified and sequenced. Sequences complementary to the 5'UTR are shown in lower-case green, and to the 3'UTR are shown in upper-case blue. A non-native nucleotide is shown in black.

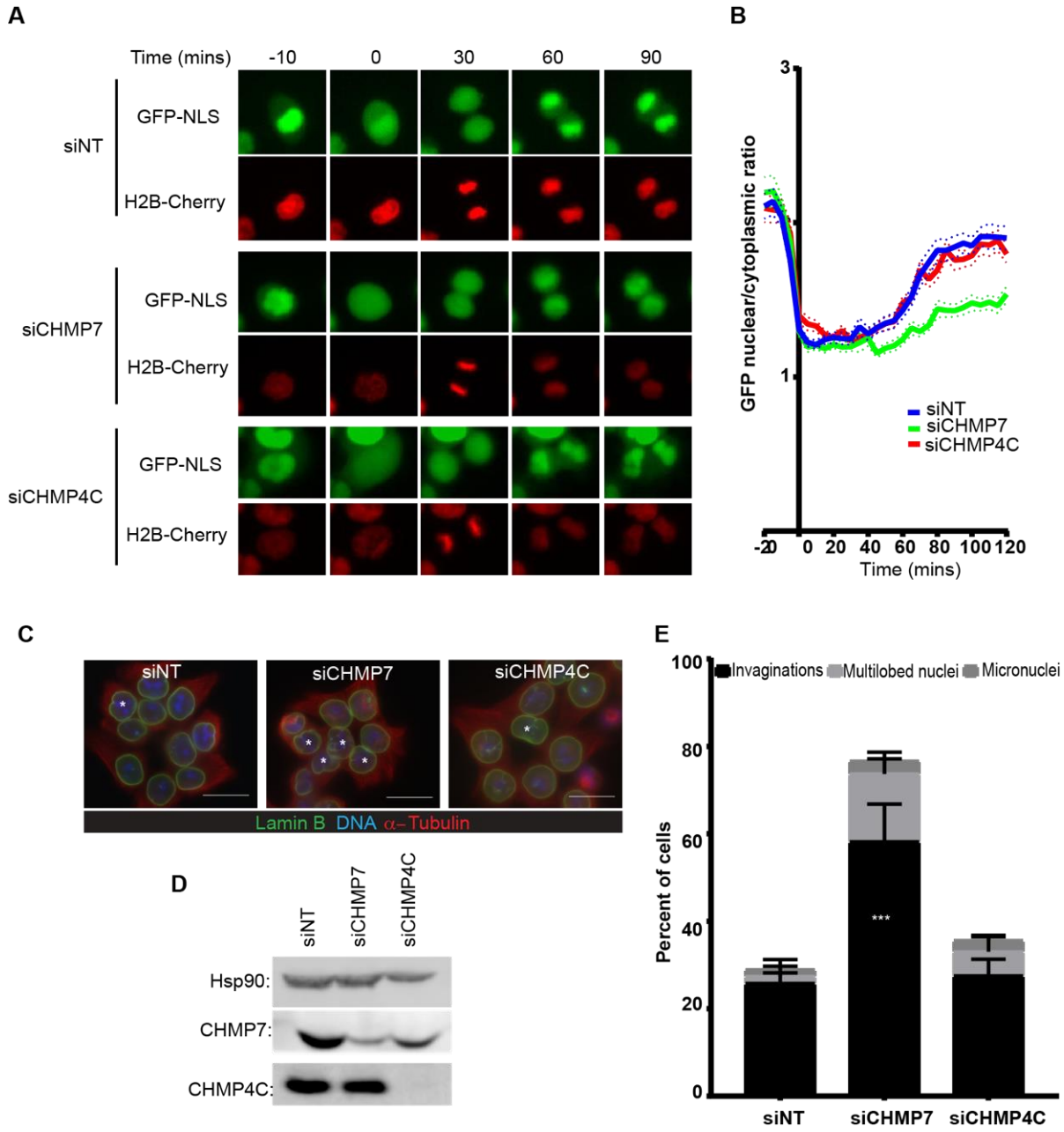

Fig S4. CHMP4C is not required for maintenance of nuclear envelope integrity.
(**A**) Time-lapse still images of nuclear GFP NLS fluorescence recovery in HCT116 cells expressing GFP-NLS, H2B-cherry and treated with the indicated siRNA. The siCHMP7 sample serves as a positive control (6). (**B**) Quantification of nuclear envelope sealing in cells treated with the indicated siRNA. Shown are mean (solid line)±SEM (dashed line) of >30 cells. Data were collected from >3 independent experiments. Movies of (A) are available in Movies S13-S15. (**C**) Cells treated with indicated siRNA stained with Lamin B (green), α tubulin, (red) and DAPI (blue). Scale bars, 20 μm. Nuclei with invaginations are marked with an asterisk. (**D**) Immunoblots showing siRNA efficiency. (**E**) Cells were categorised based on their nuclear morphology, shown are mean±SD, n>900 cells, from 3 independent experiments. *P*-value calculated using 2-way ANOVA and Sidak's multiple comparisons test comparing each category to siNT, ***P<0.001.

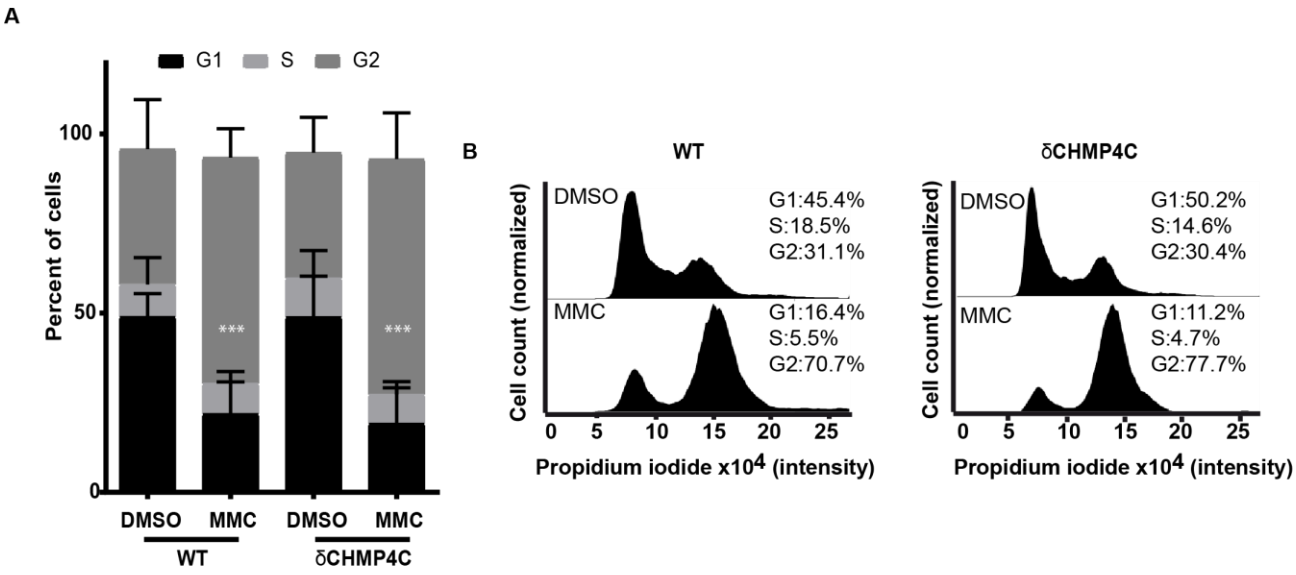

Fig S5. CHMP4C is not required for cell cycle arrest in response to DNA damage.
(**A**) Cell cycle analyses of HCT116^{WT} or HCT116$^{\delta CHMP4C}$ cells treated with either DMSO or 200 ng/mL mitomycin C (MMC) were carried out by flow cytometry following DNA staining with propidium iodide. Gating was performed manually. Shown are mean±SD of 3 separate experiments. *P*-value calculated using 2-way ANOVA and Sidak's multiple comparisons test comparing each category to siNT, ***P<0.001. (**B**) Representative cell cycle profiles of DMSO- or MMC-treated cells. Note that G2 arrest is observed in both the parental and HCT116$^{\delta CHMP4C}$ MMC-treated cells.

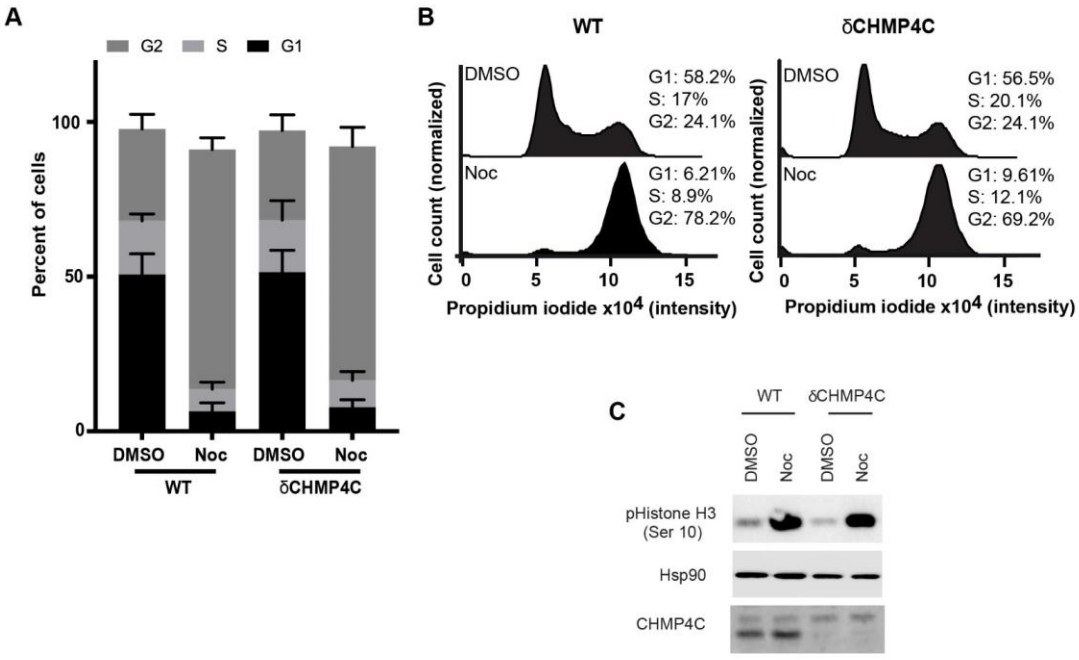

Fig. S6. CHMP4C is not required for mitotic cell cycle arrest in response to microtubule depolymerization. (**A**) Cell cycle analyses of HCT116^{WT} or HCT116$^{\delta CHMP4C}$ cells treated with either DMSO or 50 ng/mL nocodozole were carried out by flow cytometry following DNA staining with propidium iodide. Gating was performed manually. Shown are mean±SD of 3 separate experiments. (**B**) Representative cell cycle profiles of DMSO- or nocodozole-treated cells. Note that G2/M arrest is observed in both the parental and HCT116$^{\delta CHMP4C}$ nocodazole-treated cells. (**C**) Representative immunoblots showing comparable mitotic phosphorylation of Histone H3 Ser10 in response to microtubule depolymerization in HCT116^{WT} and HCT116$^{\delta CHMP4C}$.

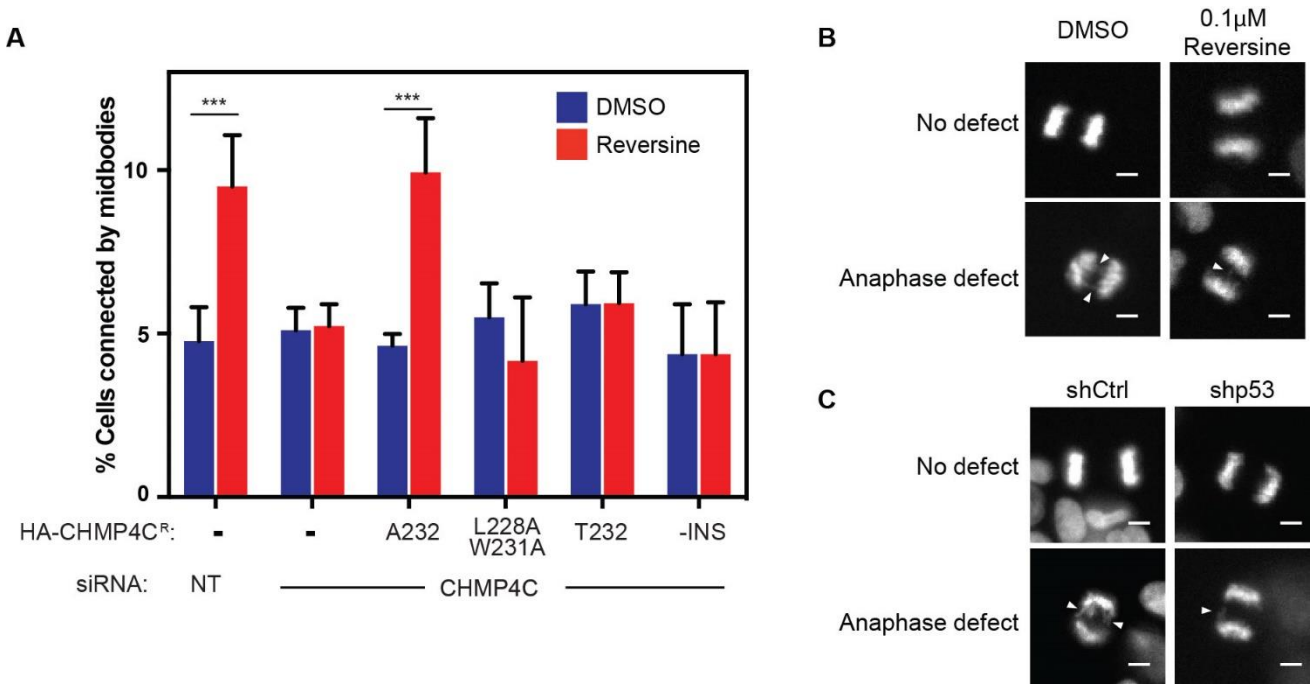

Fig. S7. Low dose reversine treatment triggers the abscission checkpoint, low dose reversine treatment or depletion of p53 induces anaphase defects.
(**A**) Cells stably expressing the indicated HA-CHMP4C construct treated with indicated siRNA for 48 hours, then with DMSO or 0.1 μM reversine for 24 hours. The number of cells connected by midbodies were scored. Data shown in (**A**) are mean±SD, n>900, from 3 independent experiments. *P*-values were calculated using 2-way ANOVA and Sidak's multiple comparisons test,***P<0.001. **(B**, **C**) Time-lapse stills of HCT116 cells stably expressing H2B-mCherry displaying normal or defective anaphases following DMSO or 0.1 μM reversine treatment (**B**) or following transduction with control or p53 shRNA (**C**), scale bars, 5 μm. Videos of anaphase cells displayed in **B**, **C** are available in **Videos 16-23**.

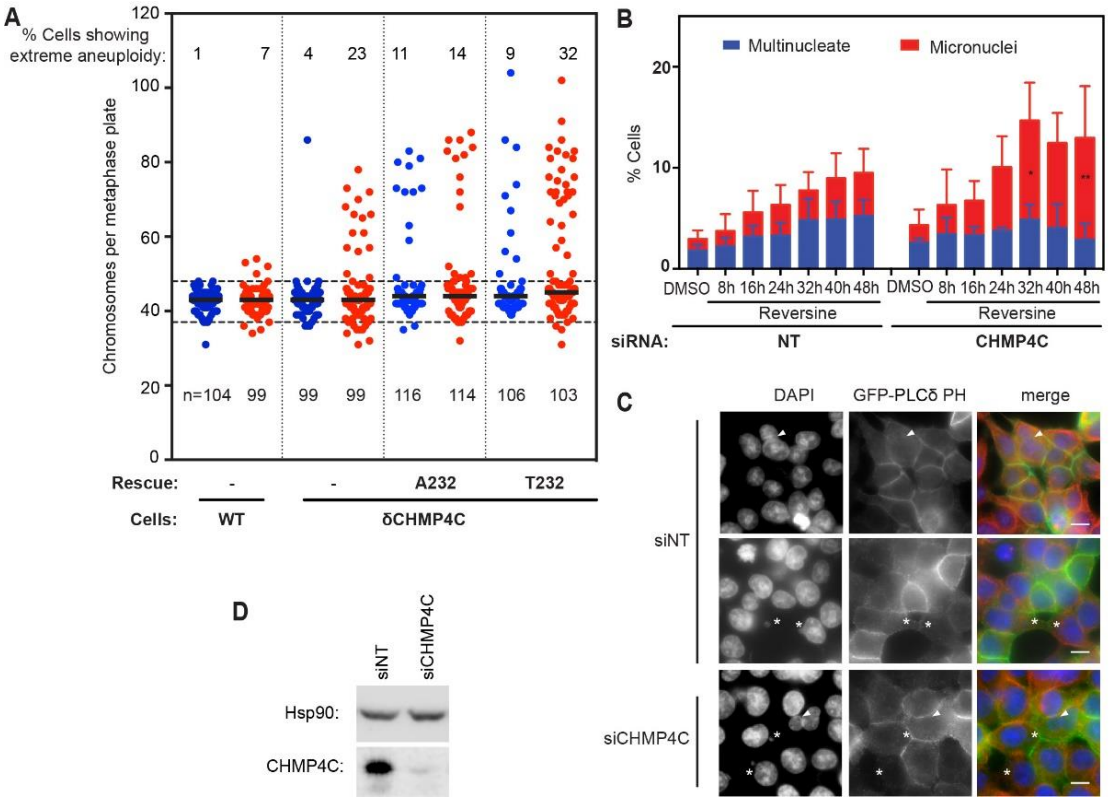

Fig. S8. Chromosomal instability in cells defective for the abscission checkpoint can be rescued by re-expression of wild-type CHMP4C and is not a consequence of cytokinesis failure and multinucleation. (**A**) HCT116^{WT} or HCT116$^{\delta CHMP4C}$ expressing the indicated HA-CHMP4C construct were cultured for 48 hours in the continuous presence of DMSO (blue) or 0.1 μM reversine (red). Metaphases were enriched by overnight treatment with nocodazole, and chromosome number was determined. Data for HCT116^{WT} and HCT116$^{\delta CHMP4C}$ are replicated from Fig. 4B. Plots show all data with medians marked with the percentage of cells displaying extreme aneuploidy indicated above the data points. Extreme aneuploidy is defined as chromosome numbers above 48 or below 37 (dashed lines). (**B,C**) HCT116 cells expressing GFP-PLCδ pleckstrin homology (PH domain) were treated with the indicated siRNA and cultured in the presence of DMSO for 48 hours or 0.1 μM reversine for the indicated times, cells were fixed and stained for GFP (green) α-tubulin (red) and DNA (DAPI, blue), scale bar, 10 μm (**C**). Cells were scored for multinucleation or the presence of micronuclei (**B**). Shown are means±SD n>1200 cells, from 4 independent experiments. *P*-values were calculated using 2-way ANOVA and Sidak's multiple comparisons test, comparing each condition to the corresponding siNT condition *=p<0.05, **=p<0.01. (**D**) Immunoblots showing siRNA efficiency from B, C.

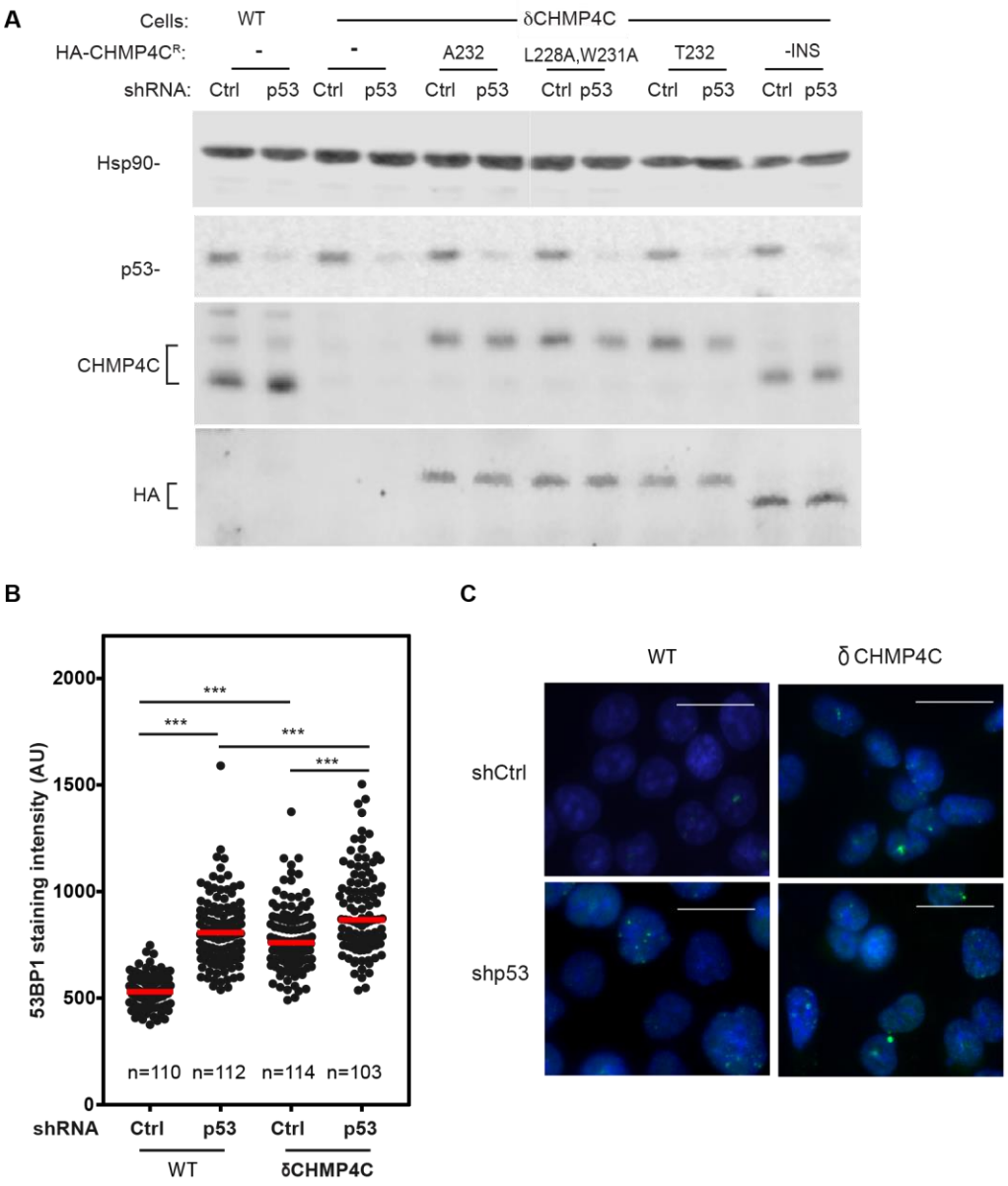

Fig. S9. The abscission checkpoint protects genomic integrity when p53 is absent.
(**A**) Representative immunoblots showing p53 depletion in parental and HCT116$^{\delta CHMP4C}$ cells stably expressing the designated HA-CHMP4C proteins. (**B**) Nuclear 53BP1 fluorescence intensity following p53 depletion in HCT116^{WT} or HCT116$^{\delta CHMP4C}$ cells. Shown are representative data from one of 4 independent experiments. Data were collected from >100 cells, mean value is marked, *P*-values calculated using one-way ANOVA,***P<0.001. (**C**) Representative immunofluorescence images from (**B**), stained with 53BP1 (green) and DNA (DAPI, blue). Scale bars are 20 µm.

Fig. 2*A*

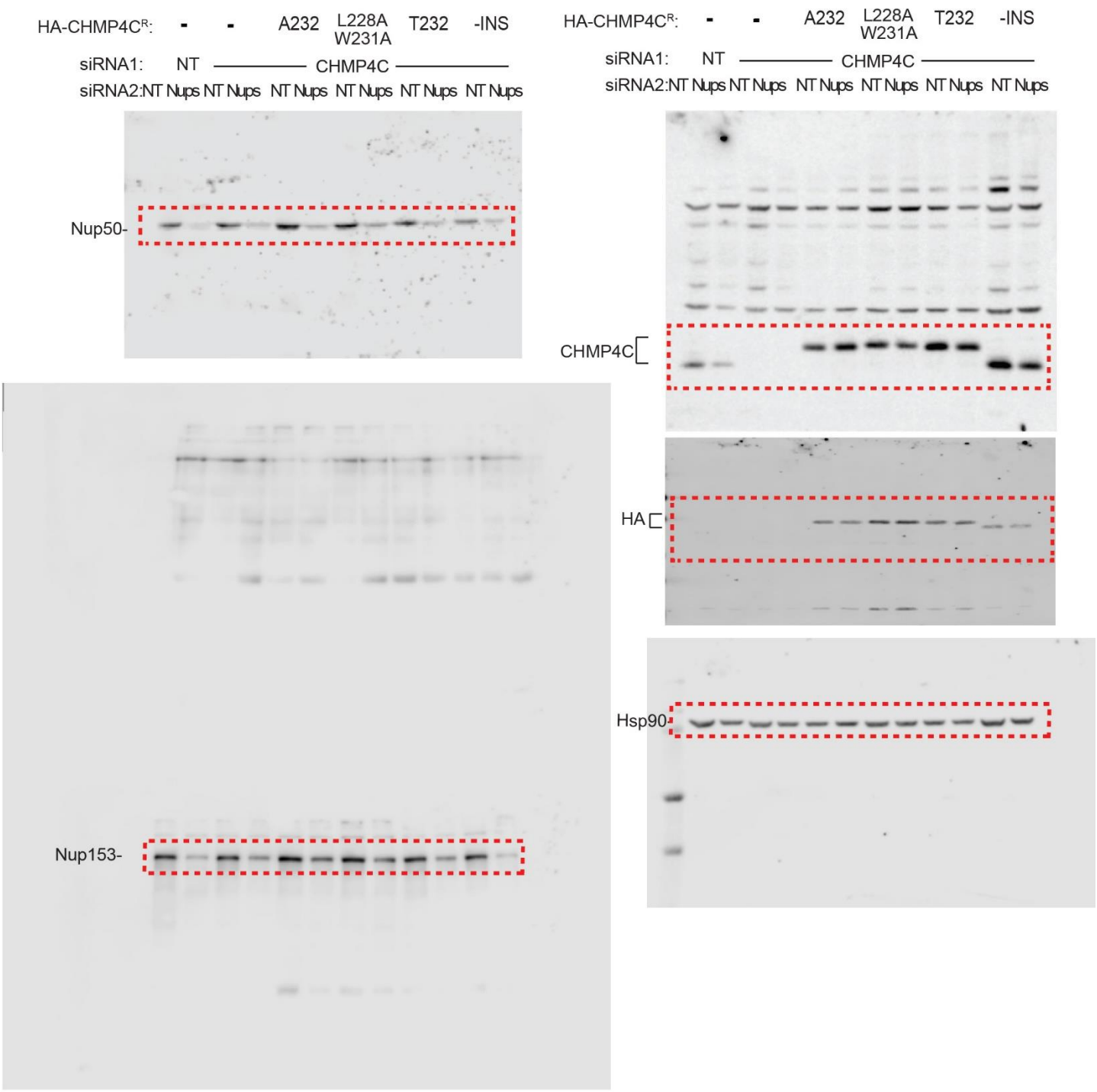
HA-CHMP4C^{R}: - - A232 L228A W231A T232 -INS
siRNA1: NT CHMP4C
siRNA2: NT Nups NT Nups NT Nups NT Nups NT Nups NT Nups
Nup50-
Nup153-
CHMP4C
HA
Hsp90-

Fig. 3*B*

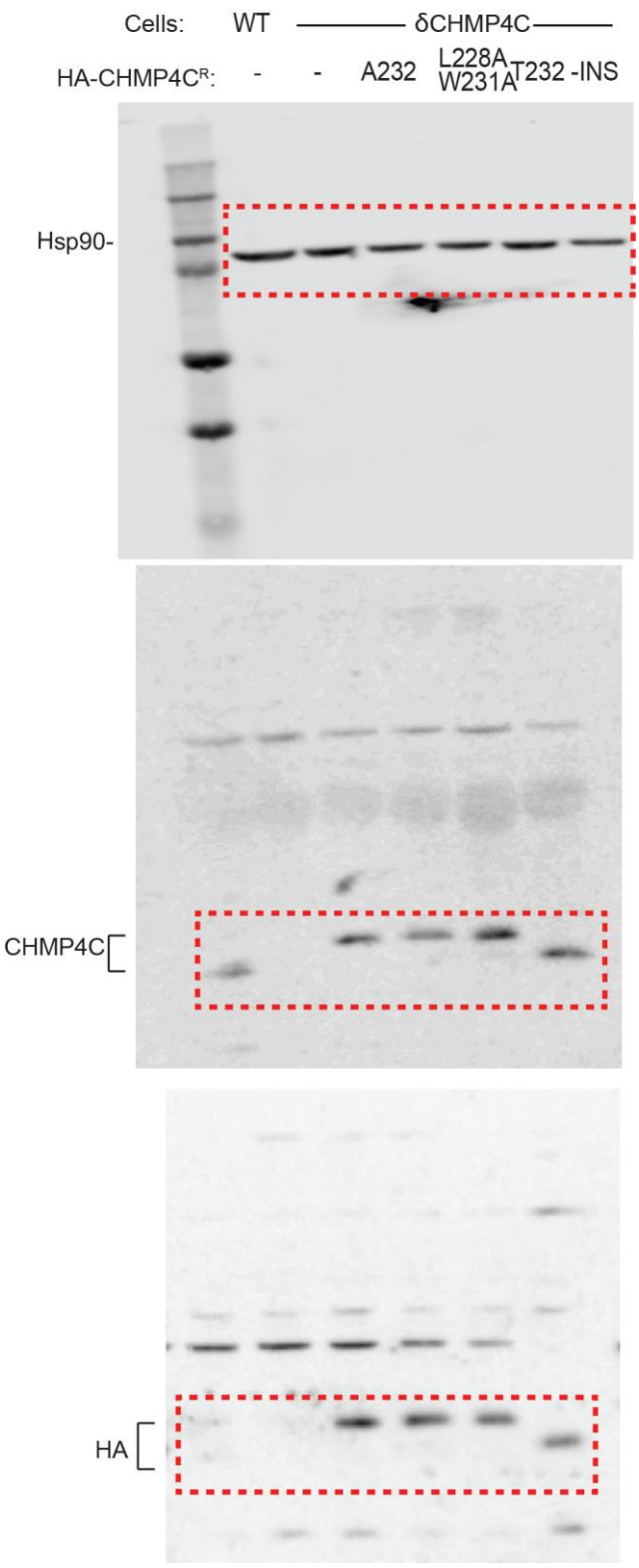
Cells:
WT
δCHMP4C
HA-CHMP4C^{R}:
-
-
A232
L228A W231A
T232 -INS
Hsp90-
CHMP4C
HA

Fig. 4*D*

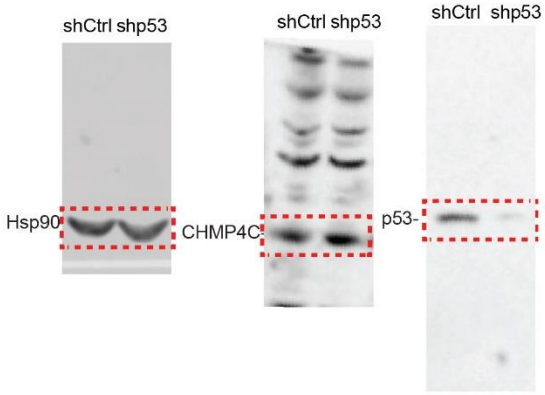

Fig. S1A

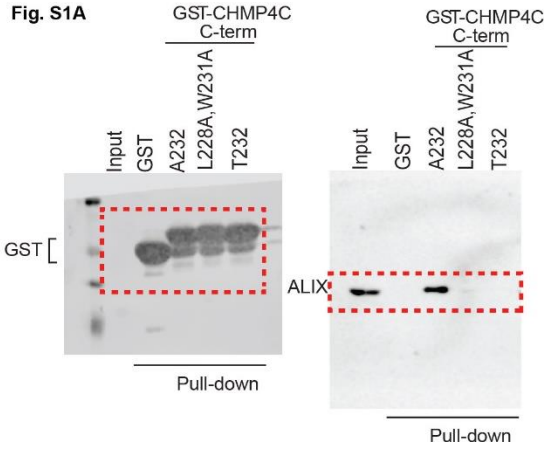

Fig. S2*B*

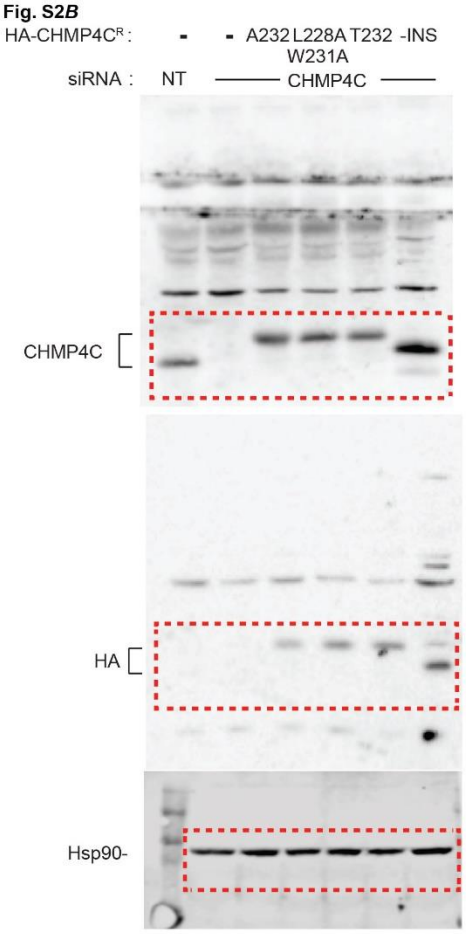

Fig. S2*C*

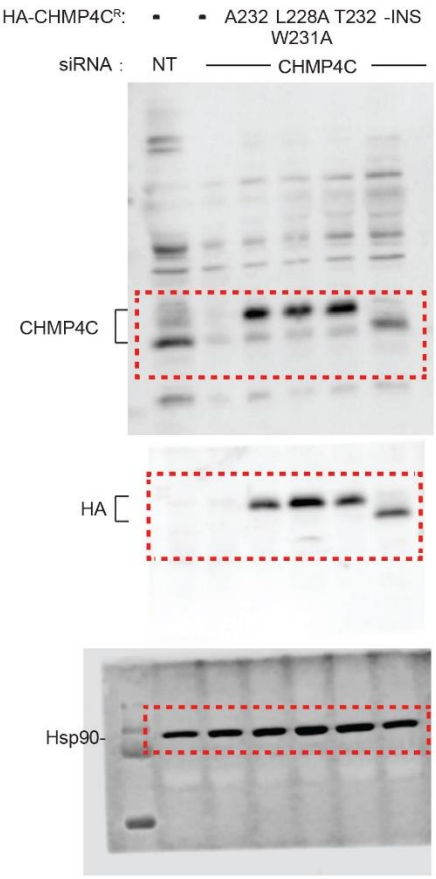

Fig. S2*D*

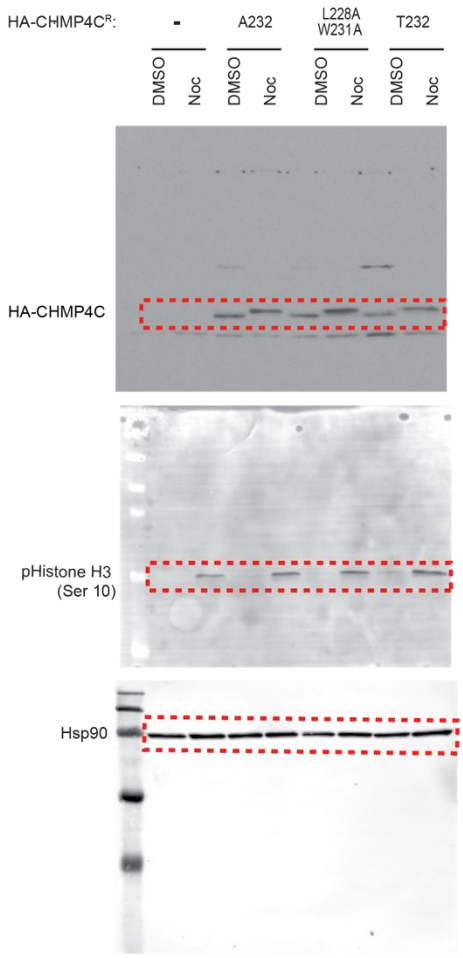

Fig. S3*D*

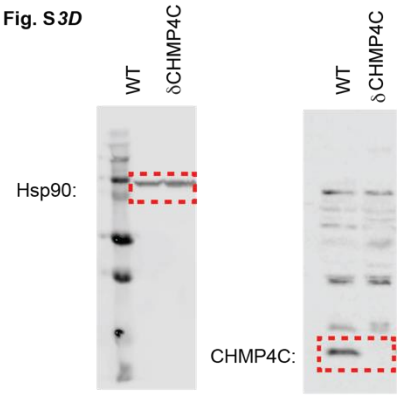

Fig. S6*C*

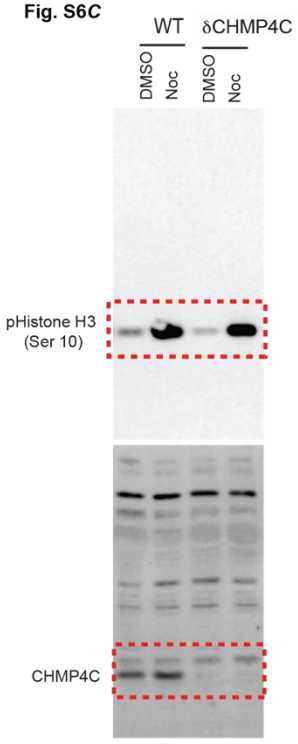

Fig. S4*D*

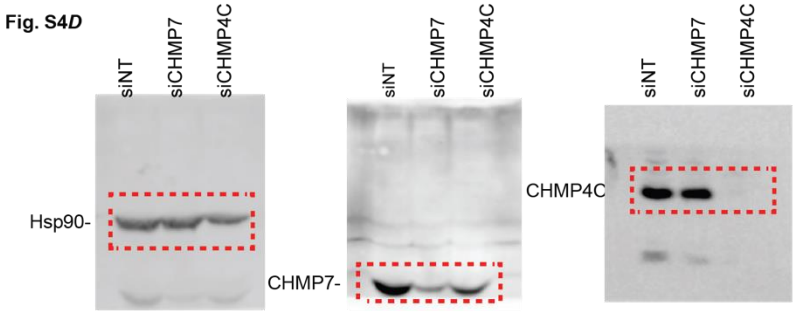

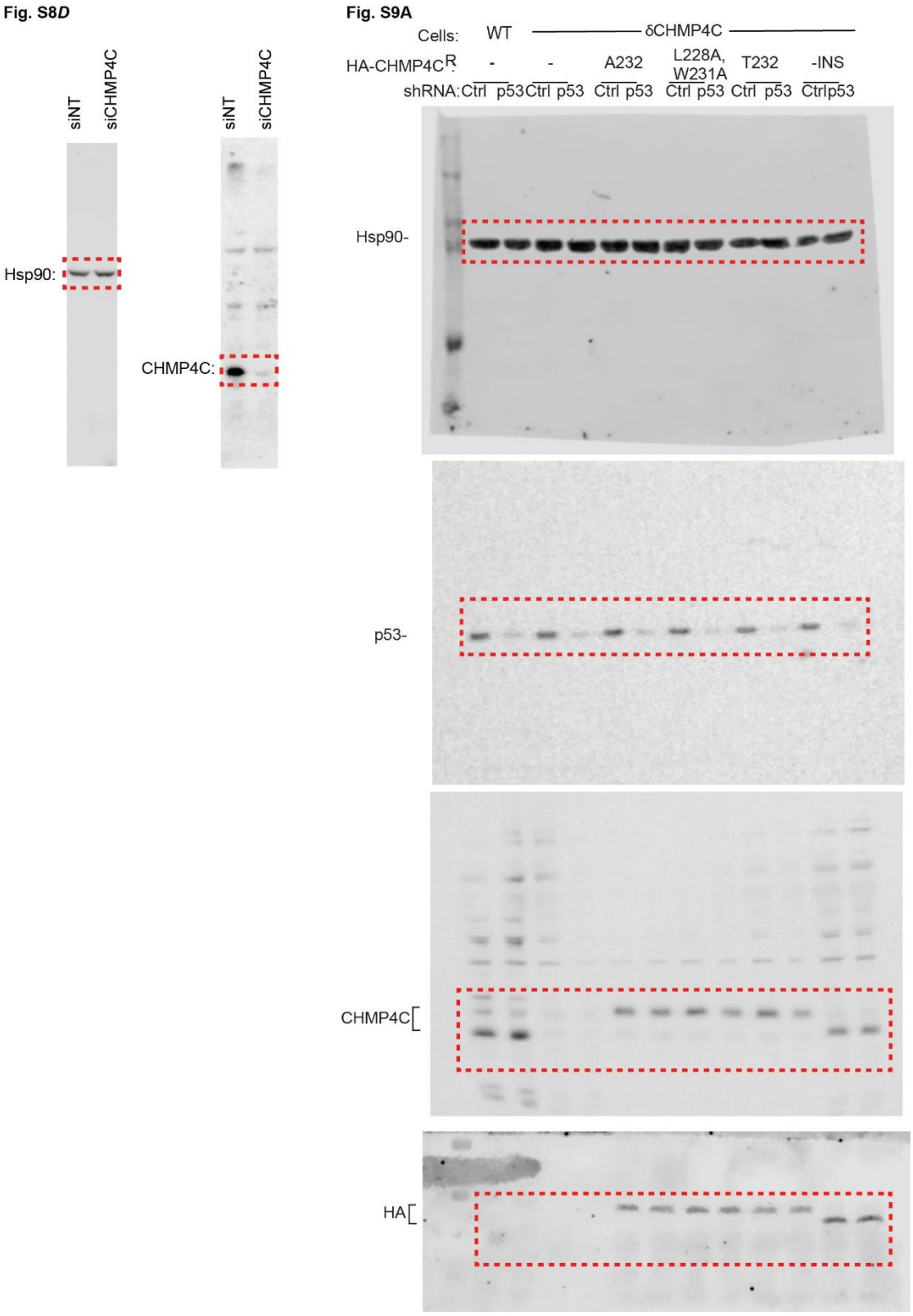

Fig S10. Unprocessed/full scans of immunoblots presented in Figs. 2, 3, 4, S1, S2, S3, S4, S6, S8 and S9.

Table S1. Data collection and refinement statistics (molecular replacement).

	ALIX / CHMP4C^{A232} (5V3R)†	ALIX /CHMP4C^{T232} (5WA1)†
Data collection		
Space group	C121	C121
Cell dimensions		
a, *b*, *c* (Å)	120.59, 60.775, 75.6538	120.979, 61.45, 76.1873
α, β, γ(°)	90, 121.558, 90	90, 121.704, 90
Resolution (Å)*	36.18-1.906 (1.974-1.906)	37.81-1.868 (1.935-1.868)
R_{merge}	0.01955 (0.5925)	0.0222 (0.808)
Total reflections	70323 (5684)	77295 (7336)
Unique reflections	35304 (2927)	38802 (3744)
R_{pim}	0.01955 (0.5925)	0.022 (0.808)
$I / \sigma I$	10.17 (1.16)	8.78 (0.97)
Completeness (%)	96.04 (77.40)	97.63 (93.38)
$CC_{1/2}$	0.996 (0.702)	0.999 (0.6)
Redundancy	2.0 (1.9)	2.0 (2.0)
Refinement		
R_{work} / R_{free}	0.1929/0.2130	0.1933/0.2147
No. atoms	3006	3010
Protein	2907	2917
Water	99	93
B-factors	66.66	75.56
Protein	67.05	76.04
Water	55.12	60.43
R.m.s. deviations		
Bond lengths (Å)	0.007	0.005
Bond angles (°)	0.82	0.72
Ramachandran Plot		
Favored (%)	97	96.2
Allowed (%)	3	3.8

† Each structure was determined using data collected from a single crystal.

*Values in parenthesis are for the highest resolution shell.

Table S2. Plasmids, antibodies and primers used in this study.

Bacterial Expression Plasmids:

Plasmid Name	Source/Reference	Internal/Addgene ID	Description
pET16b-ALIX Bro1	(1, 2)	WISP11-428/ 80641	Expresses His-ALIX residues 1-359
pET151D-TOPO-ALIX Bro1-V	(1, 2)	WISP10-648/ 80642	Expresses His-ALIX residues 1-702
pGEX 2T TEV GST			Expresses GST
pGEX 2T TEV GST-CHMP4C (216-233) A232			Expresses GST-CHMP4C (216-233) reference protein
pGEX 2T TEV GST-CHMP4C (216-233) T232			Expresses GST-CHMP4C (216-233) T232 rs35094336 mutant
pGEX 2T TEV GST-CHMP4C (216-233) L228A, W231A			Expresses GST-CHMP4C (216-233) L228A, W231A ALIX-binding mutant

Mammalian Expression Plasmids:

Plasmid Name	Source/Reference	Description
pLG2CR-CHMP4C guides	Pierre Vantiurout, Kings College London	Cas9 lentiviral vector encoding CHMP4C guide RNA sequences
pLNCX2-HA	(4)	retroviral packaging vector expressing HA empty
pLNCX2-HA-CHMP4C^{R} A232	(4)	retroviral packaging vector expressing HA-CHMP4C full length siRNA-resistant wild type, reference protein
pLNCX2-HA-CHMP4C^{R} L228A, W231A		retroviral packaging vector expressing HA-CHMP4C full length siRNA-resistant L228A, W231A ALIX-binding mutant
pLNCX2-HA-CHMP4C^{R} T232		retroviral packaging vector expressing HA-CHMP4C full length siRNA-resistant T232 rs35094336 mutant
pLNCX2-HA-CHMP4C^{R} -INS	(4)	retroviral packaging vector expressing HA-CHMP4C full length siRNA-resistant mutant lacking residues 201-217
pCMS28 H2B-mCherry		retroviral packaging vector expressing mCherry fused to H2B

pCMS28 mCherry-tubulin	(7)	retroviral packaging vector expressing mCherry-α-tubulin
pCMS28 YFP-Lap2β	(7)	retroviral packaging vector expressing YFP LAP2β residues 244-454
pNG72-GFP-NLS		retroviral packaging vector expressing GFP-Nuclear Localisation Signal derived from SV40
pNG72-GFP-PLCδ PH		Retroviral packaging vector expressing GFP fused to 2 copies of the PLCδ pleckstrin homology (PH domain) residues 1-81 separated by a linker.
pGIPZ-p53shRNA	Jesus Gil, Imperial College London	Expresses shRNA directed against p53
pGIPZ	Jesus Gil, Imperial College London	Expresses control shRNA
GagPol/pHIV 8.1		Packaging plasmids used alongside mammalian expression vector of interest and VSV-G to generate of retrovirus
pHIT VSVg		Envelope plasmid used alongside mammalian expression vector of interest and either GagPol or pHIV 8.1 to generate retrovirus

Yeast Expression Plasmids:

Plasmid Name	**Source/Reference**	**Description**
pHB18	(4)	Empty vector
pHB18-CHMP4C A232	(4)	Full length CHMP4C reference, wild type, fused to VP16 activation domain
pHB18-CHMP4C L228A, W231A		Full length CHMP4C L228A, W231A ALIX-binding mutant fused to VP16 activation domain
pHB18-CHMP4C T232		Full length CHMP4C T232 rs35094336 cancer polymorphism fused to VP16 activation domain
pGBKT7	(4)	Empty Vector
pGBKT7-CHMP4C WT	(4)	Full length CHMP4C fused to Gal4 DNA-binding domain
pGBKT7-ALIX	(4)	Full length ALIX fused to Gal4 DNA-binding domain

Antibodies:

Protein	**Organism**	**Dilution**	**Source**	**Product # (If Applicable)**

Nup153	Mouse	WB: 1:50 in 1% milk; nitrocellulose	(8)	SA1
Nup153	Mouse	WB: 1:500 in 1% milk; nitrocellulose	Biolegend	QE5
HSP90	Mouse	WB: 1:10,000 in 1% milk; nitrocellulose	Santa Cruz	F18/H-114
P53	Mouse	WB: 1:1,000 in 1% milk; nitrocellulose	Biolegend	DO-1, 645702
HA.11	Mouse	WB: 1:500 in 1% milk; nitrocellulose	Biolegend	901515
CHMP7	Rabbit	WB: 1:500 in 1% milk; nitrocellulose	Proteintech	16424-1-AP
CHMP4C	Rabbit	WB: 1:200 in 5% milk; nitrocellulose	Lampire Biologicals	N/A
GST	Mouse	WB: 1:1000 1:1000 in 1% milk; nitrocellulose	EMBL Monoclonal Antibody Production Facility	N/A
53BP1	Rabbit	IF: 1:750 in 3% FCS in 1X PBS, 0.1% Triton-X 100)	Novus Biologicals	NB 100-304
Lamin B1	Mouse	IF: 1:1,000 in 3% FCS in 1X PBS, 0.1% Triton-X 100	Abcam	119D5-F1, ab8982
ALIX	Rabbit	WB: 1:1,000 in 1% milk; nitrocellulose	Covance	UT324
Nup50	Rabbit	WB:1:500 in 1% milk; nitrocellulose	(8)	N/A
HA	Mouse	WB: 1:500 in 1% milk; nitrocellulose IF: 1:500 in 3% FCS in 1X PBS, 0.1% Triton-X 100	Cell Signaling	2367
α-tubulin	Rabbit	IF: 1:500 in3% FCS in 1X PBS, 0.1% Triton-X 100	Abcam	ab18251
α-tubulin	Mouse	IF: 1:1,000 in3% FCS in 1X PBS, 0.1% Triton-X 100	Sigma	clone DM1a
GFP	Chicken	IF: 1:1,000 in3% FCS in 1X PBS, 0.1% Triton-X 100	Abcam	ab13970
pHistone H3 Ser10	Rabbit	WB: 1:5,000 in 1% milk; nitrocellulose	Cell Signaling	9701

IF = Immunofluorescence, WB = Immunoblot; Secondary antibodies for the relevant species were IRDye680 and IRDye800 conjugated (NEB) or horseradish peroxide (HRP) conjugated (Cell Signaling).

Primers:

Name	Sense sequence
CHMP4C Primer 1	CCACAGTCTTTGTCGGTC
CHMP4C Primer 2	CACAACGTACTAGAATATCC
CHMP4C Primer 3	TCTGAGAGGGGTTGG
CHMP4C Primer4	GCATCCATTGCCCCATTCCA
GAPDH Primer 1	CTGAGGCTCCCACCTTTCTC
GAPDH Primer 2	AAGAGTTGTCAGGGCCCTTTT
CHMP4C RNA Primer 1	ATGAGCAAGTTGGGCAAGTTCTTTA
CHMP4C RNA Primer 2	TTAGGTAGCCCAAGCTGCCAATTGT
GAPDH RNA Primer 1	ATGGGGAAGGTGAAGGTCGGAGTCA
GAPDH RNA Primer 2	TTACTCCTTGGAGGCCATGTGGGCC

siRNA sequences:

Protein	Sense sequence	Source/Reference
Non-targeting	ON-TARGET plus siControl non-targeting pool	Dharmacon (D-001810-10-20)(9)
CHMP4C	CTCACTCAGATTGATGGCACA	Qiagen (Cat. number SI04279674), (4)
Nup 153	GGACUUGUUAGAUCUAGUU	Dharmacon (Custom order siRNA), (8)
Nup 50	GGAGGACGCUUUUCUGGAUTT	Dharmacon (Custom order siRNA), (8)
CHMP7	GGGAGAAGAUUGUGAAGUU	Dharmacon (Custom order siRNA), (10)

Movies S1-S6. Abscission time of HeLa mCherry-tubulin cells.

HeLa cells stably expressing the indicated HA-CHMP4C construct and mCherry-tubulin were transfected with either non-targeting or CHMP4C siRNA. Midbody resolution is indicated with an arrowhead. (**Movie S1)** siNT, abscission time, 100 minutes. (**Movie S2)** siCHMP4C, 60 minutes. (**Movie S3**) HA-CHMP4C^{A232}+siCHMP4C, 100 minutes. (**Movie S4**) HA-CHMP4C^{L228A,W231A}+siCHMP4C, 80 minutes. (**Movie S5**) HA-CHMP4C^{T232}+siCHMP4C, 80 minutes. (**Movie S6**) HA-CHMP4C^{-INS}+siCHMP4C, 80 minutes. Related to Fig. 2.

Movies S7-S12. Resolution time of YFP-Lap2β positive chromatin bridges.

HeLa cells stably expressing the indicated HA-CHMP4C construct and YFP-Lap2β were transfected with either non-targeting (**Movie S7**) or CHMP4C (**Movie S8-S12**) siRNA. Cell showing YFP-Lap2β positive bridge is marked with an arrow, and bridge resolution is indicated with an arrowhead. (**Movie S7)** siNT resolution time, 820 minutes. (**Movie S8)** siCHMP4C, 240 minutes. (**Movie S9**) HA-CHMP4C^{A232} +siCHMP4C, 540 minutes**. (Movie S10)** HA-CHMP4C^{L228A,W231A}+siCHMP4C, 220 minutes. (**Movie S11)** HA-CHMP4C^{T232}+siCHMP4C, 140 minutes. (**Movie S12)** HA-CHMP4C^{-INS}+siCHMP4C, 100 minutes. Related to Fig. 2.

Movies S13-S15. CHMP4C is not involved in mitotic nuclear envelope reformation.

Movies of stills shown in Fig. S4A. Cells stably expressing GFP-NLS and H2B-mCherry were treated with non-targeting (**Movie S13**), CHMP7 (**Movie S14**) or CHMP4C (**Movie S15**) siRNA, subjected to time-lapse microscopy and were imaged and nuclear GFP-NLS fluorescence intensity relative to cytoplasmic fluorescence intensity was determined with ImageJ. Related to Fig. S4.

Movies S16-S19. Reversine induces anaphase chromosome segregation errors.

Cells stably expressing H2B-mCherry were treated with DMSO (**Movies S16, S17**) or 0.1 μM reversine (**Movies S18, S19**) and cell division events were followed by time-lapse microscopy. Cells were scored for anaphase defects (marked with arrowhead). **Movies S16, S18** show anaphases with no defects, whereas **Movies S17, S19** show defective anaphases. Related to Fig S7B.

Movies S20-S23. p53 depletion induces anaphase chromosome segregation errors.

Cells stably expressing H2B-mChery and either control shRNA (shCtrl, **Movies S20, S21**) or shRNA against p53 (shp53, **Movies S22, S23**) were followed by time-lapse microscopy and cells were scored for anaphase defects (marked with arrowheads). **Movies S20, S22** show anaphases with no defects, whereas **Movies S21, S23** show defective anaphases. Related to Fig S7*C*.

References

1. McCullough J, Fisher RD, Whitby FG, Sundquist WI, & Hill CP (2008) ALIX-CHMP4 interactions in the human ESCRT pathway. *Proc Natl Acad Sci U S A* 105(22):7687-7691.
2. Fisher RD, *et al.* (2007) Structural and biochemical studies of ALIX/AIP1 and its role in retrovirus budding. *Cell* 128(5):841-852.
3. Studier FW (2005) Protein production by auto-induction in high density shaking cultures. *Protein Expr Purif* 41(1):207-234.
4. Carlton JG, Caballe A, Agromayor M, Kloc M, & Martin-Serrano J (2012) ESCRT-III governs the Aurora B-mediated abscission checkpoint through CHMP4C. *Science* 336(6078):220-225.

5. Ran FA, *et al.* (2013) Genome engineering using the CRISPR-Cas9 system. *Nat Protoc* 8(11):2281-2308.
6. Olmos Y, Perdrix-Rosell A, & Carlton JG (2016) Membrane Binding by CHMP7 Coordinates ESCRT-III-Dependent Nuclear Envelope Reformation. *Curr. Biol.* 26(19):2635-2641.
7. Agromayor M, *et al.* (2009) Essential role of hIST1 in cytokinesis. *Mol Biol Cell* 20(5):1374-1387.
8. Mackay DR, Makise M, & Ullman KS (2010) Defects in nuclear pore assembly lead to activation of an Aurora B-mediated abscission checkpoint. *J Cell Biol* 191(5):923-931.
9. Caballe A, *et al.* (2015) ULK3 regulates cytokinetic abscission by phosphorylating ESCRT-III proteins. *Elife* 4:e06547.
10. Morita E, *et al.* (2011) ESCRT-III protein requirements for HIV-1 budding. *Cell host & microbe* 9(3):235-242.